CHAPTER 5

Biochemistry and Localization of Somatostatin in the Retina

TADATAKA YAMADA
Department of Internal Medicine, The University of Michigan Medical School, Ann Arbor, MI 48109-0362, USA

CONTENTS

1. INTRODUCTION

In 1902 Bayliss and Starling described the first hormone, secretin, when they characterized a pancreatic stimulant that was secreted into the circulation in response to duodenal acidification. In subsequent studies this and many other hormones were identified as small polypeptides with widespread distribution throughout the body. Many of these polypeptides have been proposed as neurotransmitters in the peripheral and central nervous systems. However, the evidence for a neurotransmitter function for these peptides has been limited primarily to simple localization by immunologic means to nerve tissues. Many of the peptides in question have not been purified from nerves and thus the relationship of their immunoreactivities to chemical structures is unknown.

The complexity of the brain makes neuropeptide studies such as biosynthesis and release experiments, correlation of localization to known cellular function on the basis of electrophysiologic studies, and determination of specific cellular receptors difficult to perform as well as to interpret. The retina, however, provides an ideal system for further exploration of the neural function of brain peptides (Ames and

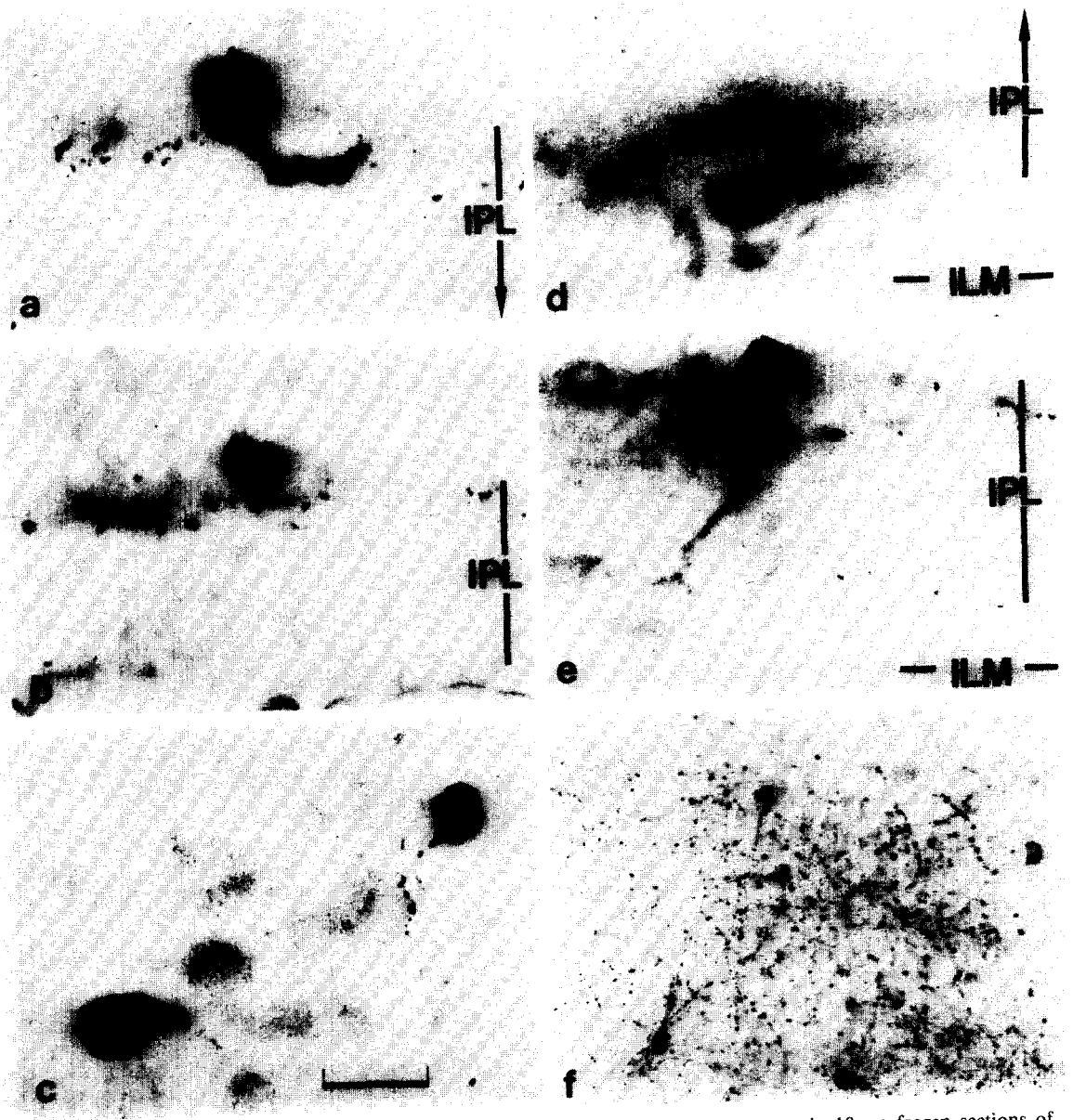

FIG. 1. SLI-containing cell bodies and processes stained by indirect immunofluorescence in 10 μm frozen sections of goldfish retina. The calibration marker in (c) represents 20 μm in (a – e) and 80 um in (f). The inner plexiform layers (IPL) are marked by the vertical lines and the inner limiting membranes (ILM) are marked by the horizonal lines. (a) Large unbranched process extending from a large round cell body (SAa1). (b) Fine varicose fibers forming a plexus in the distal IPL originating from a small spherical perikaryon (SAa2). (c) SAa1 and SAa2 cells with their processes in a tangential section, illustrating the origin of thick processes from the large cells and thin processes from the smaller cells. (d) Cell in the ganglion cell layer (SGb) associated with smooth processes. (e) Pyriform perikaryon with processes descending into the most proximal sublamina of the IPL (Sab). (f) Low-power view of tangential section of retina, illustrating the predominance of fine varicose fibers amid numerous perikarya. The names of the cell bodies containing SLI were derived as follows: S = somatostatin-containing; A = amarine cell layer, G = ganglion cell layer; a and b refer to the location of the processes in the inner plexiform layer; and 1 and 2 refer to the subtypes. Hence, SAa2 refers to somatostatin-containing cells in the amacrine cell layer of the retina with processes in sublamina a, type 2. (From Yamada *et al.*, 1980).

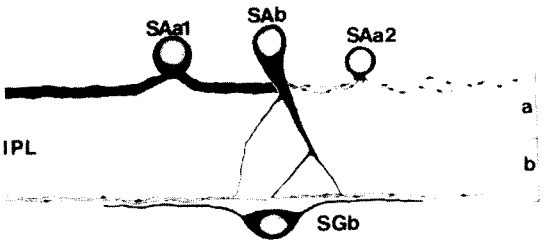

FIG. 2. Diagram of four types of SLI-containing cell bodies with their processes, Sublaminae a and b of the inner plexiform layer (IPL) are marked. (From Yamada *et al.*, 1980).

Nesbitt, 1981). It is an integral but discreet component of the brain which can be isolated without damage to its intrinsic neurons and can be maintained in organ culture for prolonged periods. Moreover, the anatomy, physiology, and pharmacology of the retina have been extensively characterized. Each of the major cell types have been studied by intracellular recording (Kaneko, 1979). Because the retina responds to light, it can be activated by the same light stimuli *in vitro* that it responds to *in vivo*. Since discreet populations of retinal cells can be activated with different light or pharmacologic stimuli, the retina provides an unique opportunity in which to perform parallel electrophysiological and biochemical studies.

For these reasons, a number of investigators initiated studies to localize neuroactive peptides in the retina. Schaeffer *et al.* (1977) first found thyrotropin releasing hormone-like immunoreactivity (TRH-LI) by radioimmunoassay in extracts of rat retina and observed that levels of this peptide increased during exposure of animals to light. Since these initial observations, a number of peptides have been localized to the retina, primarily by immunohistochemical techniques, as reviewed by Stell *et al.* (1980) and Brecha (1983). Among the peptides that my collaborators and I have examined is somatostatin.

The isolation of somatostatin was initially reported in 1973 by investigators in Guillemin's laboratory as an unexpected dividend in the search for the hypothalamic releasing factor responsible for regulation of pituitary growth hormone secretion (Brazeau *et al.*, 1973). In their early attempts to isolate thyrotropin releasing factor and luteinizing hormone releasing factor, they observed a consistent inhibition of growth hormone secretion from dispersed rat pituitary cells in culture by fractions of their hypothalamic extracts, much as Krulich *et al.* (1968) had described several years earlier. Because of the reproducibility of their findings, Brazeau *et al.* set out to purify this somatotropin-release inhibiting factor (SRIF) from a chloroform-methanol-glacial acetic acid extract of 500,000 sheep hypothalami and isolate the cyclic tetradecapeptide that we know today as somatostatin. Following these initial studies, numerous additional pharmacological actions of somatostatin were described in rapid succession, not only on pituitary hormone secretion, but on functions of such diverse organs as the pancreatic islets and the stomach. It was not until 1975, however, that Arimura *et al.* (1975) desribed the first radioimmunoassay for somatostatin and with it, the first hints as to the ubiquitous distribution of the peptide in its multiple molecular forms were provided. Today, somatostatin-like immunoreactivity (SLI) is known to be present in virtually every tissue in the body, and as aptly described by Reichlin (1983), "the names of the organisms shown to contain immunoreactive somatostatin read like the passenger's list of Noah's ark", and include not only the familiar vertebrates, but also protochordates, plants, protozoa, and even prokaryotes.

The primary evidence that somatostatin is a neurotransmitter is that somatostatin-like immunoreactivity (SLI) has been identified in axons and nerve cell bodies of primary sensory neurons (Hokflet *et al.*, 1975), sympathetic neurons (Hokfelt *et al.*, 1977), and intrinsic neurons of the intestines (Hokfelt *et al.*, 1975; Costa *et al.*, 1977), as well as in neurons of the central nervous system (Krisch, 1978). In addition, SLI has been localized to secretory granules within the median eminence (Pelletier *et al.*, 1974) and terminal synaptosomes of neurons of the hypothalamus (Epelbaum *et al.*, 1977; Styne *et al.*, 1977). SLI release from nerve tissues by depolarization has been shown to be calcium-dependent (Iverson *et al.*, 1978) and electrophysiological studies have demonstrated that somatostatin in low concentrations affects the discharge rate of neurons in various regions of the

FIG. 3. A vertical section of sublamina a of the inner plexiform layer. The edge of the original 100 μm tissue chopper section is at the left. Three labeled amacrine cell processes are marked with arrowheads. The calibration bar is 2 μm. Abbreviations: A, amacrine cell process; B, bipolar cell axon termina; G, ganglion cell dendrite; The letter symbols are used in succeeding figures. (From Marshak *et al.*, 1984).

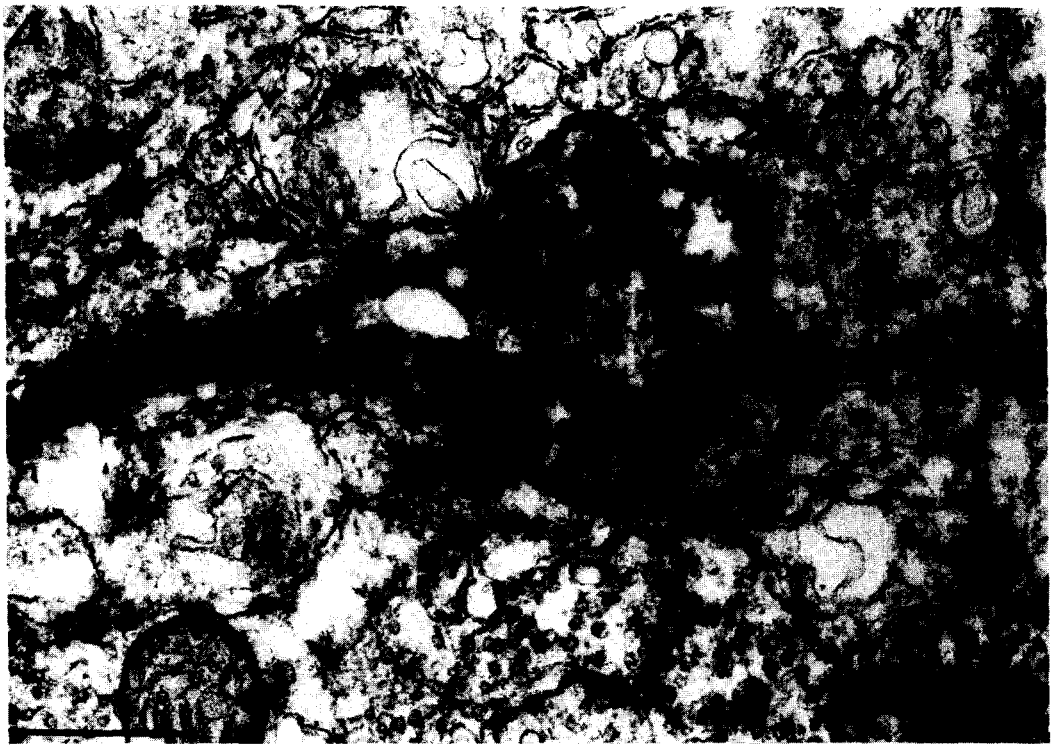

FIG. 4. A vertical section through sublamina b of the inner plexiform layer. The labeled process increased in diameter near the center of the micrograph and is presynaptic to a presumed ganglion cell dendrite (G) at the site between the arrows. The postsynaptic process did not contain any presynaptic specializations in the 12 adjacent, serial sections. The thick arrowhead indicates a large, dense-cored vesicle. The calibration bar is 0.5 μm. (From Marshak *et al.*, 1984).

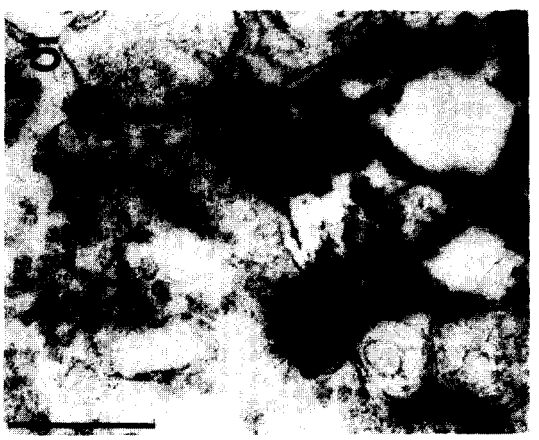

FIG. 5. A vertical section through sublamina b of the inner plexiform layer. The site of synaptic input from the labeled amacrine cell process is between the arrows. The postsynaptic cell was identified as a bipolar cell by its characteristic indented shape, high synaptic vesicle density, high cytoplasmic electron density, and synaptic ribbon (arrowhead). The calibration bar is 1 μm. (From Marshak *et al.*, 1984).

FIG. 6. A vertical section through sublamina a of the inner plexiform layer. The synaptic ribbon (arrowhead) of this bipolar cell axon terminal has been sectioned tangentially. This terminal is presynaptic to the labeled amacrine cell process below. The calibration bar is 0.5 μm. (From Marshak *et al.*, 1984).

FIG. 7. A tangential section through sublamina a of the inner plexiform layer. A bipolar cell telodendron receives a synapse from a labeled amacrine cell process at the site between the arrows. This telodendron was traced to the terminal of a large, mixed, rod-cone bipolar cell in adjacent sections. The calibration bar is 1 μm. BT, bipolar cell telodendron. (From Marshak *et al.*, 1984).

FIG. 9. A vertical section through sublamina a of the inner plexiform layer. The unlabeled amacrine cell process contains a few small, electron-lucent vesicles which are not clustered near the site, between the arrowheads, where it receives a synaptic contact from the labeled amacrine cell process. The calibration bar is 0.5 μm. As, amacrine cell soma. (From Marshak *et al.*, 1984).

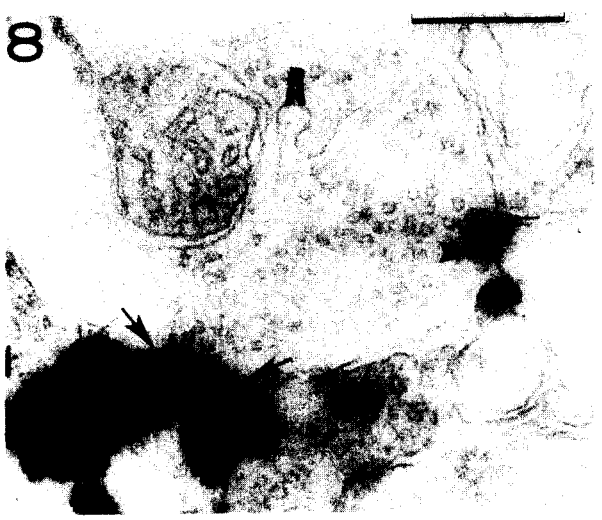

FIG. 8. A vertical section through sublamina b of the inner plexiform layer. The amacrine cell contains small, electron-lucent vesicles, which are clustered at the arrowhead, where it is presynaptic to an unlabeled process and near the site between the arrows, where it is presynaptic to the labeled amacrine cell process. The calibration bar is 0.5 μm. (From Marshak *et al.*, 1984).

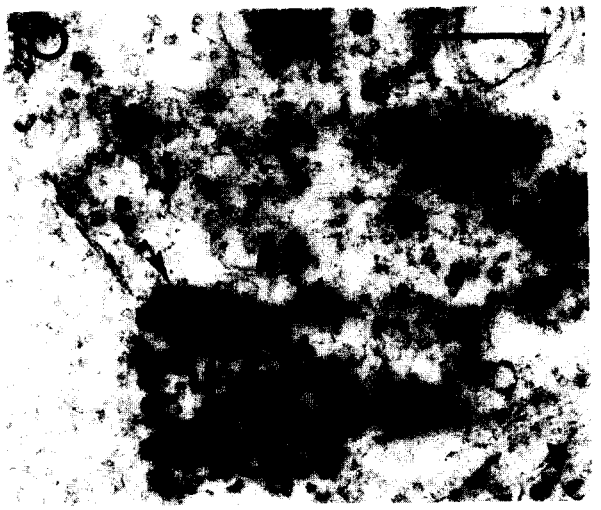

FIG. 10. A vertical section through the border between the inner nuclear and inner plexiform layers. The soma of this amacrine cell was identified by its position in the most proximal row of the inner nuclear layer. It receives a synaptic contact from the labeled amacrine cell process at the site between the arrows. The arrowhead indicates unlabeled, large, dense-cored vesicles in an adjacent process. The calibration bar is 0.5 μm. (From Marshak *et al.*, 1984).

TABLE. 1. *Identified Synapses of Amacrine Cells Containing SLI**

Type to SLI cells	Sublamina a	Sublamina b
Presynaptic		
Bipolar	2 (12%)	1 (11%)
Amacrine	15 (88%)	8 (89%)
Postsynaptic		
Bipolar	2 (5%)	2 (8%)
Amacrine	23 (53%)	15 (58%)
Ganglion	18 (42%)	9 (35%)

*Table 1 summarizes 95 identified synapses made by labeled cells — 31 from serial sections in the tangential plane and 64 from serial sections in the vertical plane. In each column the number of contacts of each type observed is given followed in parentheses by the percentage of the total presynaptic or postsynaptic in that sublamina. (From Marshak *et al.*, 1984).

brain (Dodd and Kelly, 1978; Ioffe *et al.*, 1978; Renand *et al.*, 1975), dorsal horn of the spinal cord (Randic and Miletic, 1978), and myenteric plexus of the intestines (Guillemin, 1976). Furthermore, a system for rapid sequestration and degradation of somatostatin has been identified in brain capillaries (Pardridge *et al.*, 1985).

During the past several years my principal collaborators (David Marshak, Scott Basinger, and Mimi Takami) and I have concentrated on extending our initial description of SLI in discreet cells in the amacrine cell layer of the retina (Yamada *et al.*, 1980) to ultrastructional characterization of the SLI-containing retinal cell (Marshak *et al.*, 1986), examination of the pathways of SLI biosynthesis (Yamada and Basinger, 1982), and characterization (Marshak *et al.*, 1984) and isolation of retinal SLI (Marshak *et al.*, 1983; Takami *et al.*, 1985). We hope that these studies will provide the groundwork upon which future physiological studies with somatostatin peptides of known structure can be undertaken by ourselves as well as by others. In addition, we hope that our observations have shed light on the nature of somatostatin molecular biology by providing an understanding of the pathways of post-translational processing of the somatostatin precursor.

2. LOCALIZATION

2.1. Light Microscopy

Although SLI has been found in retinas from a variety of species (Stell *et al.*, 1980; Brecha, 1983), this review will focus on the localization of SLI in the goldfish since extensive characterization of SLI-containing neurons in the retina at both the light and electronmicroscopic level has only been achieved in these species.

For light microscopic studies, the enucleated eyes of light-adapted goldfish were sectioned longitudinally through the optic disc and those of dark-adapted fish were sectioned equatorially. The retinas were dissected free and fixed in 4% (wt/vol.) paraformaldehyde in a phosphate-buffered saline (PBS) solution (0.05M sodium phosphate, 0.4M NaCl, pH 7.2) for 16 hr. After incubation in 30% sucrose in PBS for 24 hr, the tissues were frozen, then 10μm sections were obtained and mounted on gelatin-coated slides. The sucrose was removed by rinsing in PBS and the specimens were incubated for 2 hr at 37° with somatostatin antisera and then for 30 min in fluorescein isothiocyanate conjugated goat anti-rabbit gamma globulin. Appropriate controls were obtained with non-immune rabbit serum or somatostatin antiserum absorbed with 60 μM somatostatin. After rinsing in PBS, the slides were mounted in glycerol/PBS (3:1, vol.:vol.) and examined by epi-illumination.

As depicted in Fig. 1, 3 distinct SLI-containing cell types were identified in the amacrine cell layer of the goldfish retina and a fourth was identified in the ganglion cell layer. In addition, a prominent plexus of fine varicose fibers interspersed with larger unbranched processes 2 – 3 μm in diameter was identified with the somatostatin antiserum in the distal half of the outer sublamina (sublamina a) of the inner plexiform layer (Figs 1a, b, and f). Two types of processes descended to the inner sublamina of the inner plexiform layer (sublamina b) where they formed a second plexus. One of these types was relatively thick (1 μm in diameter at the base) and arborized as it coursed through the inner plexiform layer; the other was thin and did not arborize (Fig. 1e).

Approximately 5% of the proximal row of cells in the inner nuclear layer contained SLI and there were 3 primary types. One type (SAa1) had large round perikarya with thick smooth processes that extended laterally in sublamina a of the inner plexiform layer (Figs 1a and c). The fine varicose processes in this sublamina could be traced to

TABLE. 2. *Concentrations of Somatostatin-like Immunoreactivity in Extracts of Retinas from a Variety of Vertebrate Species*

	SLI (pmol)			
Species	Per gram	Per retina	Per gram	Per retina
Goldfish	13.6	4.0		3.5 (R)
Carp	1.6	0.5		
Frog	9.8	0.5		
Chicken	25.3	3.5	62.2 (E)	7.5 (BU)
Rat	7.5	0.20	31.7 (E)	0.20 (E)
				0.41 (R)
				0.68 (S)
				0.82 (L)
Rabbit	4.3	0.16	4.3 (E)	
Hog	9.8	1.9		
Cow	39.4	15.1	29.9 (E)	

Data obtained in our laboratory are listed on the left. The hog and rabbit retinas were extracted in acid/acetone; the rest were extracted in 3% acetic acid. Results from other laboratories are listed on the right. BU = Buckerfield *et al.*, 1981; E = Eskay *et al.*, 1980; L = Lake and Patel, 1980; R = Rorstad *et al.*, 1979, 1981; and S = Shapiro *et al.*, 1979.

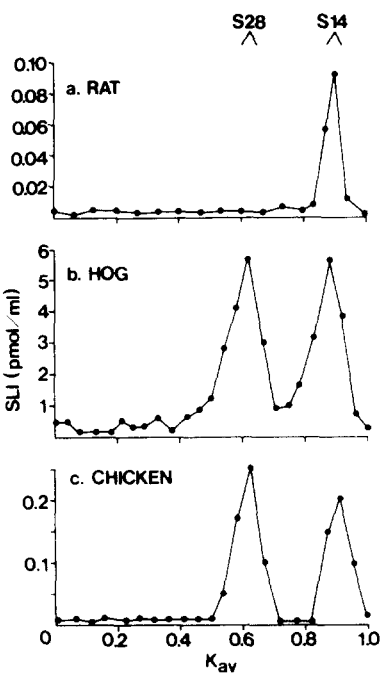

FIG. 11. Sephadex G50 sf chromatography of retinal extracts from rat (a), hog (b), and chicken (c). The elution volume (V_e) had been expressed as K_{av} (equal to $V_e - V_o / V_t - V_o$) to normalize for differences in column size. The columns were calibrated by noting the elution volume of NaCl (V_t), bovine serum albumin (V_o), somatostatin-14 (S14) and somatostatin-28 (S28). (From Marshak and Yamada, 1984).

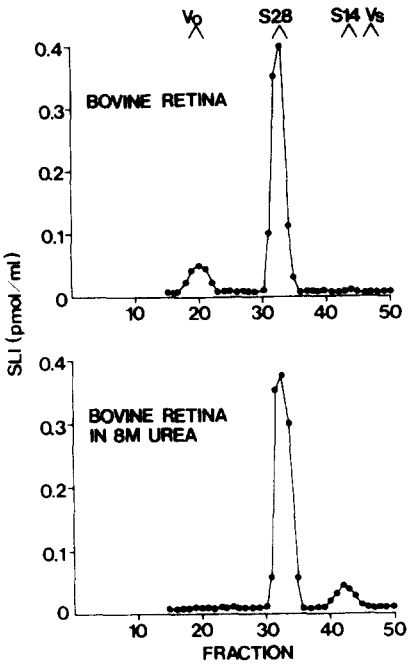

FIG. 12. Sephadex G50 chromatography of bovine retinal extracts. Extracts were chromatographed before and after 1 hr of incubation in 8 M urea. Both samples were applied to the same column (1 × 120 cm) of Sephadex G50 sf equilibrated in 0.1 M ammonium acetate, pH 5.0. Each 2 ml fraction that was eluted was assayed for SLI. The column was calibrated as noted in Fig. 11. (From Marshak and Yamada, 1984).

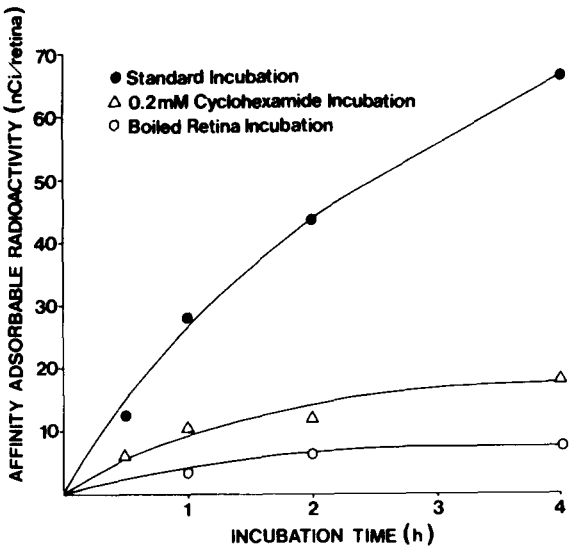

FIG. 13. Incorporation of (^{35}S)cysteine by frog retinas into material adsorbable with somatostatin-affinity column. Three sets of 10 retinas were pulse-labeled in medium containing (^{35}S)cysteine (47.6 μCi/ml) One set of retinas was boiled prior to incubation; another set was preincubated for 15 min as well as pulse-labeled in medium containing 0.2 mM cycloheximide, and the third set was incubated in standard fashion. At 0, 0.5, 1, 2, and 4 hr, two retinas were removed from pulse medium and extracted with 3% acetic acid. The neutralized extracts were applied to somatostatin-affinity column and eluted with 10% acetic acid. The affinity eluates were counted in a liquid scintillation spectrometer. (From Yamada and Basinger, 1982).

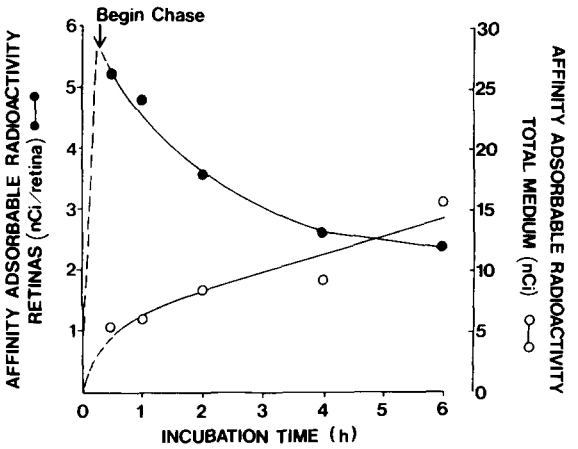

FIG. 14. Disappearance of affinity-adsorbable radioactivity from pulse-labeled retinas following chase-incubation in radioactivity-free medium. A set of 10 retinas was pulse-labeled with (^{35}S)cysteine for 15 min and transferred to nonradioactive chase medium. At 15, 45, 105, 225, and 345 min of chase incubation (0.5, 1, 2, 4, and 6 hr of total incubation), two retinas and 1 ml of medium were removed, extracted, subjected to affinity chromatography, and assayed for radioactivity. The affinity-adsorbable radioactivity of each milliliter of medium was multiplied by the total volume of medium present in the incubation mixture at the time it was sampled to obtain a value for total affinity-adsorbable radioactivity in the medium. (From Yamada and Basinger, 1982).

originate from a second cell type (SAa2) that had smaller spherical perikarya (Fig. 1b). A third cell type (SAb) had large pyriform perikarya with both thick and thin processes that descended to sublamina b of the inner plexiform layer (Fig. 1e). The possibility that this cell type also gave rise to the thin varicose processes in sublamina a could not be excluded. One cell type (SGb) with somewhat flattened perikarya in the outermost layer of the ganglion cell layer (Fig. 1d) was also identified as containing SLI. It gave rise to fine smooth processes that extended along the most proximal portion of sublamina b of the inner plexiform layer. The various SLI-containing cells of the goldfish retina and their processes are depicted in schematic form in Fig. 2.

2.2. Electronmicroscopy

To characterize the ultrastructure of the processes of SLI containing neurons in the retina and examine their synaptic connections, we extended our immunohistochemical studies to the electronmicroscopic level. For these studies goldfish retinas were fixed in 4% paraformaldehyde and 0.05% glutaraldehyde, embedded in 1% low-gelling temperature agarose and 100 μm sections were cut and labeled using the peroxidase-antiperoxidase method. Serial ultrathin (10 μm) sections were collected on copper grids and then coated with carbon and photographed.

Since the sections examined for electron-microscopy were obtained at random, largely from the inner plexiform layer (Fig. 3), the majority of labeled fibers represented the beaded dendrites of the SAa2 and SAb type SLI cells. Both the thin portion and the bulbous swellings associated with these processes are depicted in Fig. 4. The synapses, as demonstrated in this figure, were identified as the parallel, straight, widely spaced, and electron dense portions of the opposing membranes on the pre- and post-synaptic cells.

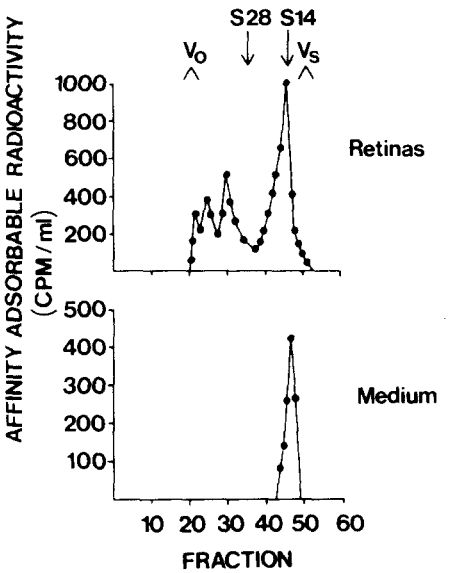

FIG. 15. Chromatographic elution of affinity-adsorbable radioactivity in retinal extracts and in chase medium. After a 30 min pulse-labeling in (^{35}S)cysteine-containing medium, and a 30 min incubation in 30 ml of chase medium, a set of six retinas was incubated in 2 ml of fresh chase medium for an additional 30 min. The retinas and medium were then extracted and affinity-adsorbed, and the affinity eluate was applied to a Sephadex G50 (superfine) column (1 × 120 cm) and eluted with 0.1 M ammonium acetate, pH 5.0. Aliquots of eluted 2.2 ml fractions were assayed for radioactivity. The columns were calibrated by elution of bovine serum albumin (V_o), NaCl (V_s), somatostatin 14 (S14), and somatostatin 28 (S28). (From Yamada and Basinger, 1982).

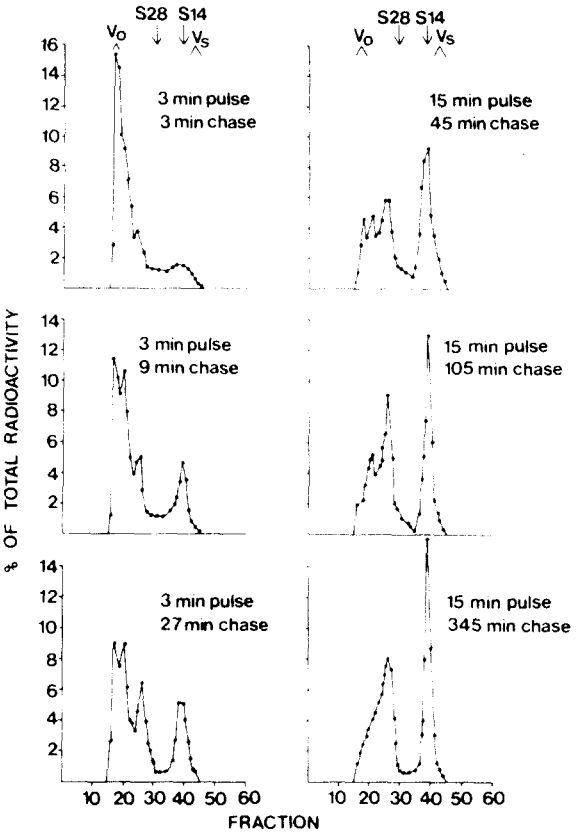

FIG. 16. Change in chromatographic elution pattern of affinity-adsorbable radioactivity obtained from retinas pulse-labeled with (^{35}S)cysteine for 3 min and then incubated in chase medium for 3, 9 or 27 min, or pulse-labeled for 15 min and incubated in chase medium for 45, 105, or 345 min. The affinity eluates were chromatographed on a Sephadex G50 (superfine) column as described in Fig. 15 and fractions were assayed for radioactivity. (From Yamada and Basinger, 1982).

Some labeled processes also contained large dense-cored vesicles but these were not localized in the area adjacent to the pre-synaptic specialization. Other smaller vesicles with electron-luscent centers were also distributed throughout the processes but appeared to cluster at sites of synaptic specialization. Synaptic junctions between dendrites of various SLI containing cells and those of the other cells with processes in the inner plexiform layer are depicted in Figs 5 – 10. After examining a large number of sections, we observed that SLI containing retinal processes both received most of their synaptic inputs from and extended most of their outgoing synapses to other amacrine cells (Table 1). However, a substantial number of contacts were also made with ganglion cells and, to a lesser extent, bipolar cells. Of particular note was that the pattern of synapses did not differ between processes in sublamina a and b.

3. CHARACTERIZATION OF MOLECULAR FORMS

3.1. Contents of SLI

For initial biochemical characterization, we examined the contents and molecular forms of SLI in the retinas of a variety of species. Whole retinas were obtained from freshly killed animals

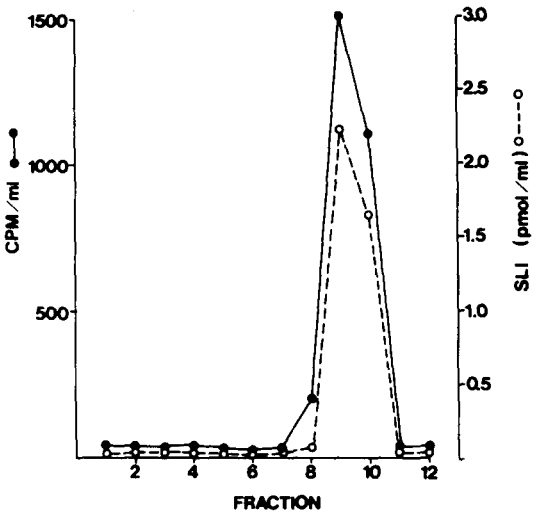

FIG 17. Elution of biosynthetic (^{35}S)SLI peak IV (see Fig. 15) and synthetic somatostatin-14 on high pressure liquid chromatography using a uBondapak C18 column (0.39 × 30 cm). Fractions (1 ml) were eluted isocratically with 29% acetonitrile in 0.1% trifluoroacetic acid at a flow rate of 1 ml/min. (From Yamada and Basinger, 1982).

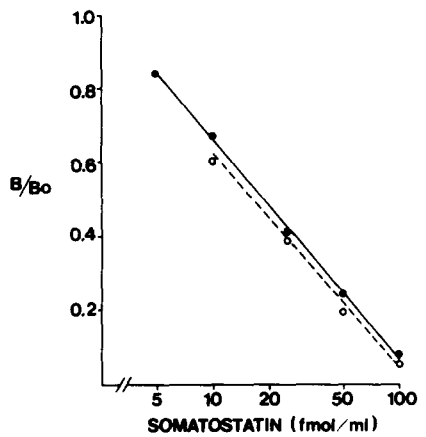

FIG. 18. Displacement of biosynthetic (^{35}S)SLI peak IV (O-see Fig. 15) and ^{125}I-Tyr^{1}-somatostatin (●) from anti-somatostatin antibody in the presence of increasing concentrations of unlabeled somatostatin-14. Displacement is expressed as a ratio of bound counts at any given unlabeled somatostatin concentration (B) to bound counts in the absence of added somatostatin (B_o). (From Yamada and Basinger, 1982).

and extracted in 3% acetic acid. In a few instances, extractions were also performed using acetone (70%) in 3% acetic acid. The recovery of somatostatin-14 (S14) or somatostatin-28 exogeneously added to the retinas before the extraction process averaged 90–100%. After extraction, aliquots were applied to gel chromatography on Sephadex G50 superfine columns equilibrated and eluted with either 0.1 M ammonium acetate pH 5.0 or 1% acetic acid. Each eluted fraction and the original extracts were analyzed for SLI by radioimmunoassay using an antiserum (Ab 1001) that is specific for the ring portion of S14 and cross-reacts 50% with S28.

The concentrations of SLI in various vertebrate retinas is depicted on Table 2. The data obtained in our laboratory generally were comparable to those reported by others. Of particular note was the high concentration of SLI present in bovine retina, an observation that proved to be useful when the purification of retinal SLI was undertaken (*vide infra*). It was of great interest that species as closely related as goldfish and carp had such widely varying concentrations of retinal SLI, but similar differences have been reported between *Rana catesbiana* and *Rana pipiens* (Eskay *et al.*, 1980).

3.2. Molecular Forms

As in many other tissues, SLI was present in 2 major molecular forms, one that corresponded to S14 and the other that corresponded to S28 (Fig. 11). In the case of bovine retina, another molecular form eluted as a larger molecule than S28 but gel filtration of the extracts under dissociative conditions revealed this to be a artifact caused by non-covalent association of S14 with an unidentified macromolecule (Fig. 12). The species differences in distribution of SLI into the two major molecular forms were remarkable. Whereas most of the species studied had both S28 and S14 forms, the rat had only the latter, while virtually all of the bovine retinal SLI was the former. These differences may reflect differences in post-translational processing of the somatostatin precursor in the retinas of the 2 species.

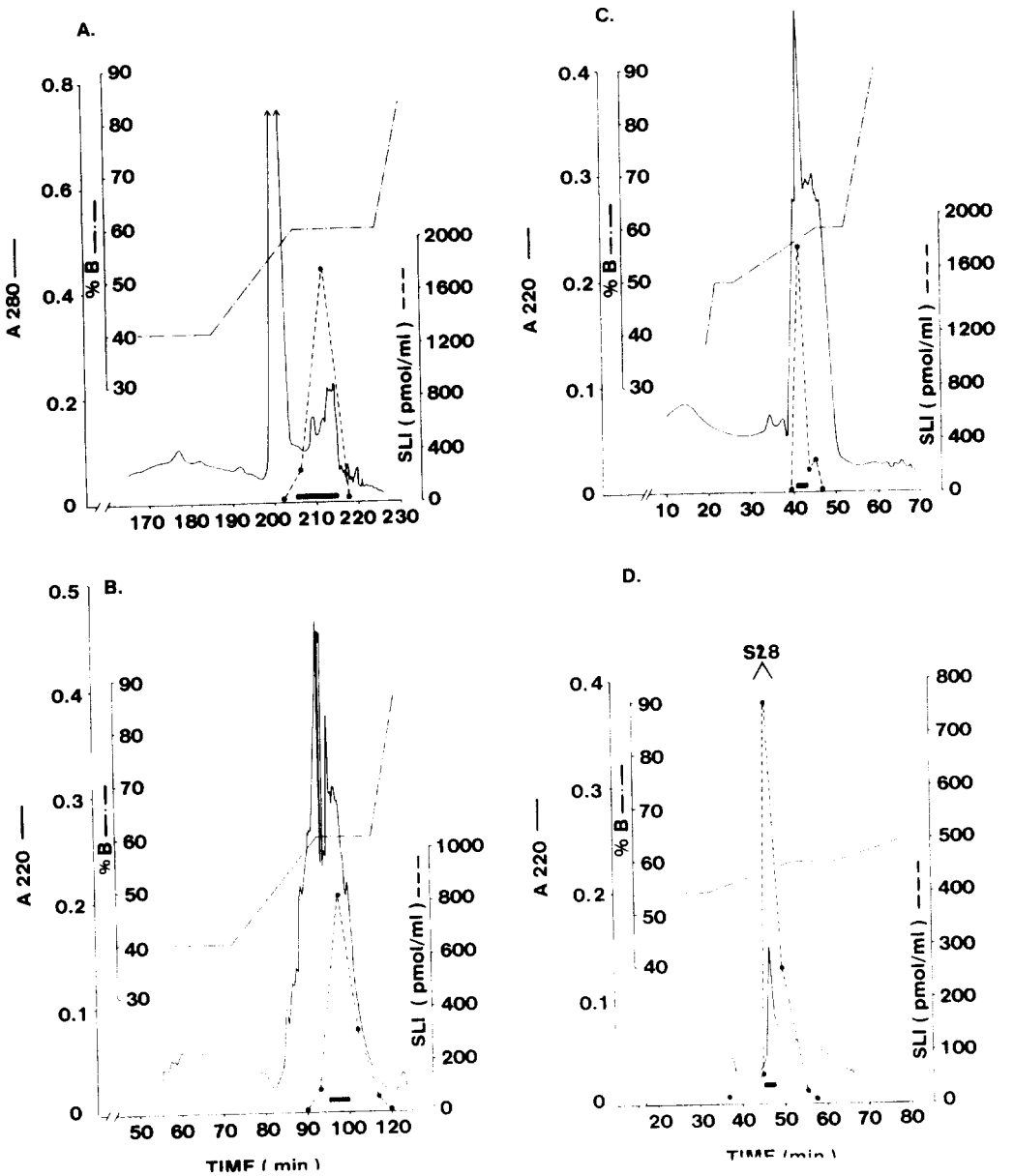

FIG. 19. Purification of bovine retinal somatostatin-like immunoreactivity (SLI) by high-pressure chromatography. After extraction with 3% acetic acid and purification by affinity chromatography, bovine retinal SLI was applied sequentially to high-pressure liquid chromatography on reverse-phase C-18 (A) and phenyl columns (B – D). The columns were equilibrated in 0.1% trifluoroacetic acid then eluted with a stepwise gradient of 50% acetonitrile in 0.1% trifluoroacetic acid (buffer B) as indicated in each figure. A280 (A) or A220 (B – D) was monitored with a variable wavelength detector, and SLI in each fraction was quantified by radioimmunoassay. The fractions pooled for further purification (A – C) or amino acid sequencing (D) are indicated by the black bars. The elution position of synthetic somatostatin octacosapeptide (S28) is indicated in D. (From Marshak *et al.*, 1983).

TABLE. 3. *Recovery of Bovine Retinal SLI at each Step of Purification*

Step	SLI (nmol)	Recovery (%) Step	Recovery (%) Cumulative	Purification (X)
Extract	18.6	–	100.0	1
Affinity	19.3/11.8*	~100.0	~100.0	150
HPLC (C – 18)	9.0	76.0	76.0	16,500
HPLC (Phenyl #) 3.8	42.2	42.2	32.2	46,000
HPLC (Phenyl #2)	2.7	71.1	22.8	82,000
HPLC (Phenyl #3)	1.7	62.9	14.4	103,000

*Only 11.8 nmol of the total SLI was used for further purification; the rest was stored for future analysis. (From Marshak *et al.*, 1983).

TABLE 4. *Amino Acid Sequences of Purified Somatostatin*

	1	2	3	4	5	6	7	8	9	10	11	12	13	14
Somatostatin 28	Ser-	Ala-	Asn-	Ser-	Asn-	Pro-	Ala-	Met-	Ala-	Pro-	Arg-	Glu-	Arg-	Lys
Bovine Retinal SLI														
Somatostatin 25														
Somatostatin 22							Asp-	Asn-	Thr-	Val-	Thr-	Ser-	Lys-	Pro

	15	16	17	18	19	20	21	22	23	24	25	26	27	28
Somatostatin 28	Ala-	Gly-	Cys-	Lys-	Asn-	Phe-	Phe-	Trp-	Lys-	Thr-	Phe-	Thr-	Ser-	Cys
Bovine Retinal SLI			(Cys)								(Phe, Thr, Ser, Cys)			
Somatostatin 25														
Somatostatin 22	Leu	Asn		Met		Tyr				Ser-	Arg		Ala	
Somatostatin 14														

From Marshek *et al.*, 1983.

TABLE 5. *Amino Acid Composition of Bovine Retinal Somatostatin*

Amino acid	Experimental	Expected
His	0.1 (0)	0
Lys	3.0 (3)	3
Trp*	0.0 (0)	1
Arg	1.6 (2)	2
Asx	4.3 (4)	3
Thr	2.1 (2)	2
Ser	3.1 (3)	3
Glx	2.2 (2)	1
Pro	3.0 (3)	2
Gly	2.2 (2)	1
Ala	3.9 (4)	4
1/2Cys*	0.9 (1)	2
Val	0.0 (0)	0
Met	0.5 (1)	1
Ile	0.4 (0)	0
Leu	0.4 (0)	0
Tyr	0.2 (0)	0
Phe	2.8 (3)	3

*Under these hydrolysis conditions the recoveries of Cys and Trp are low. From Marshak *et al.*, 1983.

4. BIOSYNTHESIS OF SLI

4.1. Label Uptake and Release

In order to confirm that the SLI present in the retina represented the products of local peptide synthesis, and to gain insight into the post-translational processing of somatostatin precursors, we undertook biosynthetic studies. For these experiments we used the frog retina because of its usefulness as a model for electrophysiological studies. The strategy employed for these studies was first to incorporate radioactive tracer amino acids into newly synthesized SLI, and then to immunoimmobilize the synthetic product for quantitative and qualitative studies.

Retinas were stripped free of pigmented epithelium and removed in the dark from groups of dark-adapted frogs (*Rana pipiens*). The retinas were then incubated in Krebs – Ringer buffer containing 8 μg/ml penicillin, 12 μg/ml

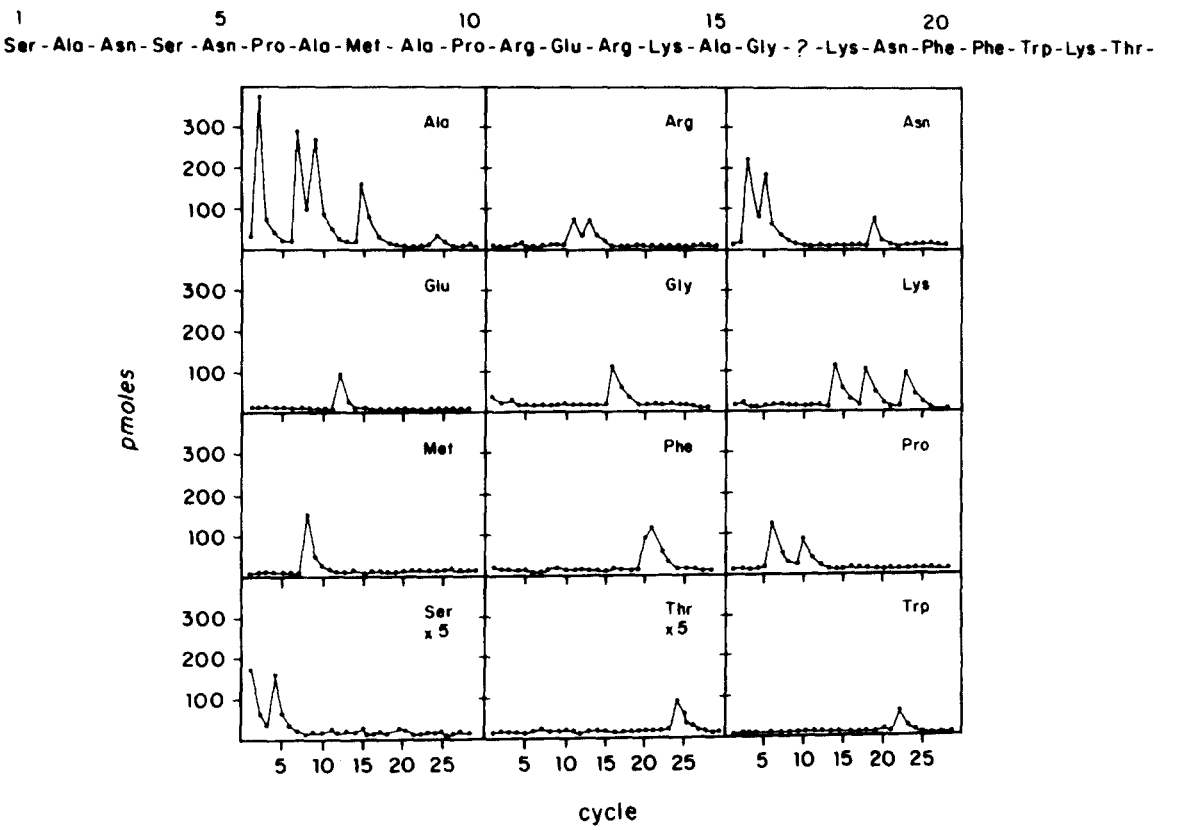

FIG. 20. Yields of phenylthiohydantoin derivatives of amino acids derived from bovine retinal somatostatin by automatic Edman degradation. Approximately 3.0 nmol peptide (as estimated by amino acid analysis) were applied, but yield of the amino-terminal serine was only 380 pmol (12.7%). Yields were calculated by comparison with standard after normalization for recovery, with diethylphthalate as an internal marker. Unmeasurable yields prevented amino acid sequencing beyond threonine in the 24th cycle. The absence of a clearly identifiable derivative in the 17th cycle is consistent with the presence of half-cysteine, which is not detected unless the native disulfide bond is chemically modified. (From Marshak *et al.*, 1983).

streptomycin, 200 kallikrein inhibitory units/ml Trasylol (FBA Pharmaceuticals, New York), and 47.6 μCi/ml ^{35}S-cysteine (564 Ci/mmol, New England Nuclear, Boston, Massachusetts). Following a 3 or 15 minute incubation in pulse medium, the retinas were transferred, after thorough washing, to chase incubation medium containing unlabeled L-cysteine (0.16 mM) and casamino acids (10 μg/ml). At various time intervals 2 retinas and 1 ml of culture medium were removed, extracted in 3% acetic acid and neutralized. The samples were then applied to an affinity column made with anti-somatostatin antibody (7812) linked to Affi-Gel 10. The bound radioactivity was eluted with 10% acetic acid and counted in a liquid scintillation spectrometer. The affinity eluates were then chromatographed on a Sephadex G50 superfine column (1 × 120 cm) and eluted with 0.1 M ammonium acetate buffer, pH 5.0.

As depicted on Fig. 13 affinity absorbable radioactivity (presumably newly synthesized SLI) gradually increased over the 4 hr duration of the study and this increase could be inhibited by nearly 75% with cycloheximide, indicating that it involved a conventional ribosomal process. During the first hour, roughly 28 μCi of ^{35}S-cysteine was incorporated into SLI. Based on the specific activity of the label and assuming that at least one molecule of label was incorporated into each molecule of SLI, we calculated the basal rate of SLI synthesis to approximate 25 fmol/retina/hr.

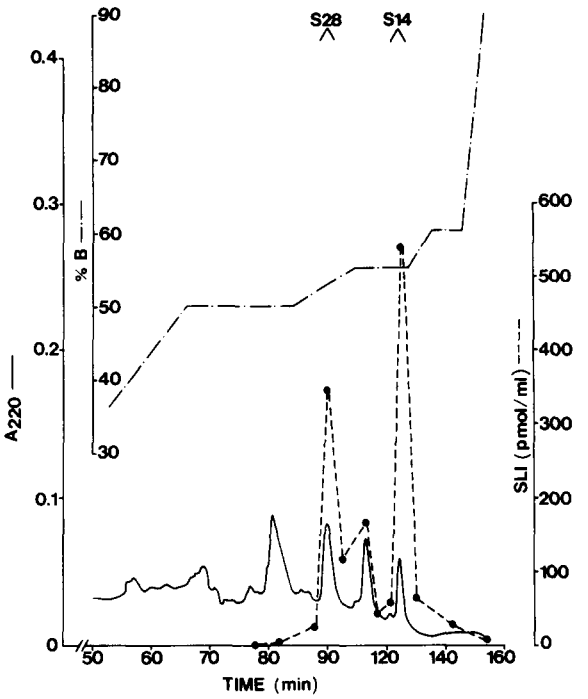

FIG. 21. Elution profile on reverse-phase phenyl high-pressure liquid chromatography of SLI purified from bovine brain. Purification was achieved according to the protocol described in Fig. 19. The gradient profile is indicated. The elution positions of synthetic somatostatin tetradecapeptide (S14) and S28 are indicated at the top of the figure. (From Marshak and Yamada, 1983).

Since the total SLI content in frog retinas is roughly 500 fmol/retina, the turnover rate of retinal SLI in the basal state appears quite low.

When pulse-chase studies were performed, affinity adsorbable radioactivity in the retinas gradually decreased with time of incubation in chase medium (Fig. 14). A complementary increase in radioactivity was observed in the culture medium. Roughly 85% of total affinity-adsorbable radioactivity was recovered when the specific radioactivity of the retinas and medium were summated. This indicates that the turnover of SLI in unstimulated retinas can be accounted for largely by the basal release of the peptide. Radioactivity from the retinal extracts eluted from Sephadex G50 in 4 distinct peaks: one in the void volume (peak I, K_{av} = 0.00), another which co-eluted with synthetic somatostatin 14 (peak IV, K_{av} = 0.84) and two intermediate in location (peaks II, K_{av} = 0.12; and III, K_{av} = 0.32) (Fig. 15). In contrast, only the peak corresponding to S14 was secreted into the culture medium. This observation is particularly important since it indicates that the radioactivity appearing in the medium did not derive from leakage of intracellular contents but from selective release of peptide. The apparently selective release of S14 despite the synthesis of other forms of SLI is curious but has been observed in other somatostatin biosynthetic systems (Chiba *et al.*, 1987).

4.2. Post-Translational Processing of SLI

When the chromatographic elution profile of SLI was examined over the time course of a pulse-chase experiment the distribution of radioactivity gradually shifted over time from peaks I and II to peaks III and IV (Fig. 16). However, no evidence of a shift of counts from peak III (corresponding to S28) to peak IV (corresponding to S14) was observed. Over 90% of radioactivity in pools of each of the peaks could be immunoprecipitated by incubation with anti-somatostatin antibody and goat anti-rabbit gamma globulin. Furthermore, the biochemical identity of peak IV was further confirmed by showing its co-elution with S14 on high pressure liquid chromatography (HPLC) (Fig. 17) and its parallel displacement with the standard curve by S14 in radioimmunoassay (Fig. 18). These findings suggest that the small molecular form of SLI synthesized in the retina is indistinguishable from S14 and, furthermore, that it does not derive from further post-translational modification of S28. The shift in radioactivity from the 2 larger peaks (I and II) to the two smaller peaks (III and IV) suggests the presence of 2 precursor forms. We cannot confirm whether the smaller precursor form (peak II) represents a processing product derived from peak I or an independently synthesized precursor. The absence of these larger molecular forms of SLI on gel filtration of standard-tissue extracts may result from their relatively rapid conversion to smaller molecular forms which, in turn, accumulate in substantial quantities because of their slow turnover.

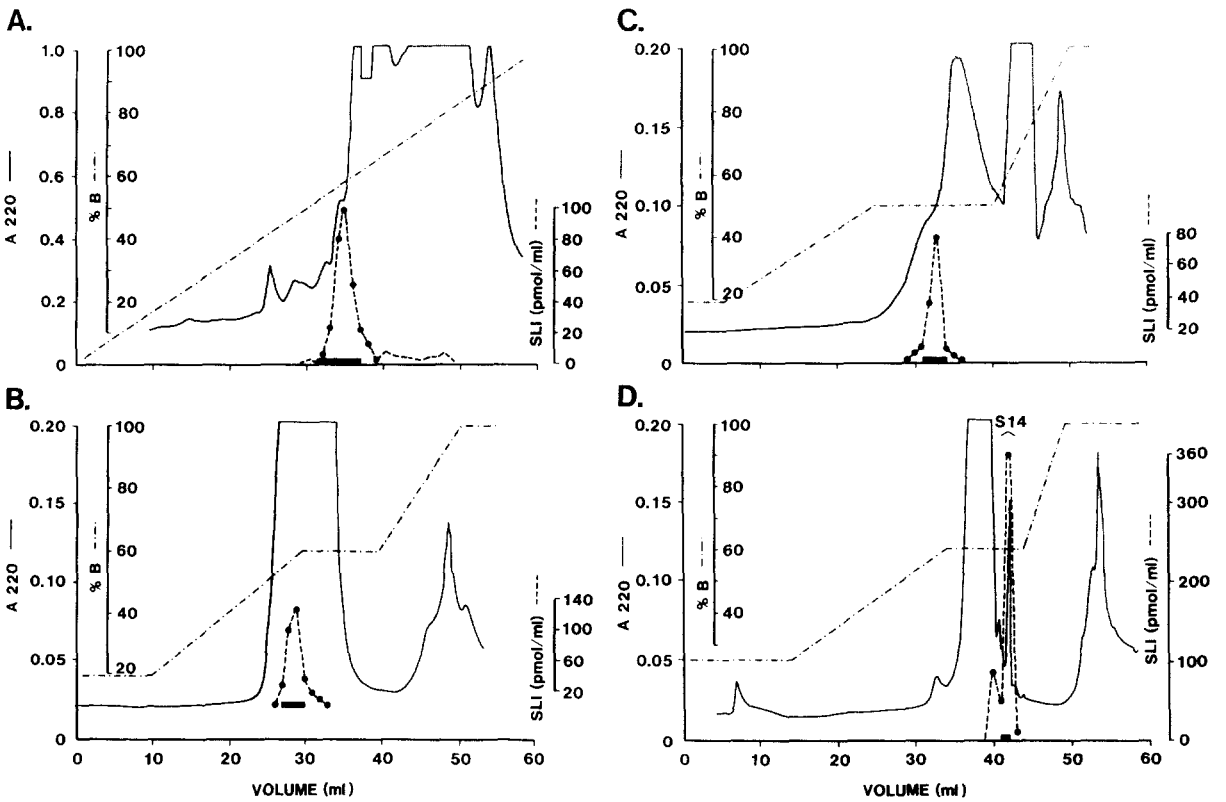

FIG. 22. Purification of frog brain SLI by HPLC. After extraction with 3% acetic acid and purification by affinity chromatography, frog brain SLI was subjected to HPLC on reverse-phase C-18 Z-Module (A – C) and Vydac (D) columns. The columns were equilibrated in 0.1% TFA and then eluted with a stepwise gradient of 50% acetonitrile in 0.1% TFA (buffer B) as indicated in each panel. A_{220} was monitored, and the SLI in each fraction was quantified by radioimmunoassay. The fractions pooled for further purification (A – C) or amino acid sequencing (D) are indicated by the black bars. The elution position of synthetic S14 as indicated in D. (From Takami *et al.*, 1985).

5. STRUCTURE OF RETINAL SOMATOSTATIN

5.1. Bovine Retina

In order to provide biochemical confirmation of the immunochemical studies in the retina, we undertook the purification of retinal SLI. Determination of the correct amino acid sequences for retinal SLI is also an essential prerequisite for interpretation of physiological studies. In examining a variety of vertebrate retinas for SLI as noted above, we observed large differences in SLI concentration even among closely related species. However, on a unit basis, it was clear that the bovine retina would be the most practical source for purification of retinal SLI. In contrast to the retinas of frogs, goldfish, chickens and hogs which contain roughly equal amounts of SLI comparable to S14 and S28, nearly all of the bovine retinal SLI co-eluted with S28 on Sephadex G50 column chromatography. For purification 3000 freshly obtained bovine retinas were extracted in boiling 3% acetic acid and the neutralized extracts were applied to chromatography on affinity beads made by linking anti-somatostatin antibody to Affi-Gel 10 beads. The beads were washed sequentially with distilled water, 0.1 M ammonium acetate pH 5.0, and 4 M guanidine HCl, then the immobilized SLI was eluted with 2% trifluoroacetic acid. The affinity eluates were further purified by HPLC in a μ-Bondapak C18 column and three sequential μ-Bondapak phenyl columns using various gradients of acetonitrile in

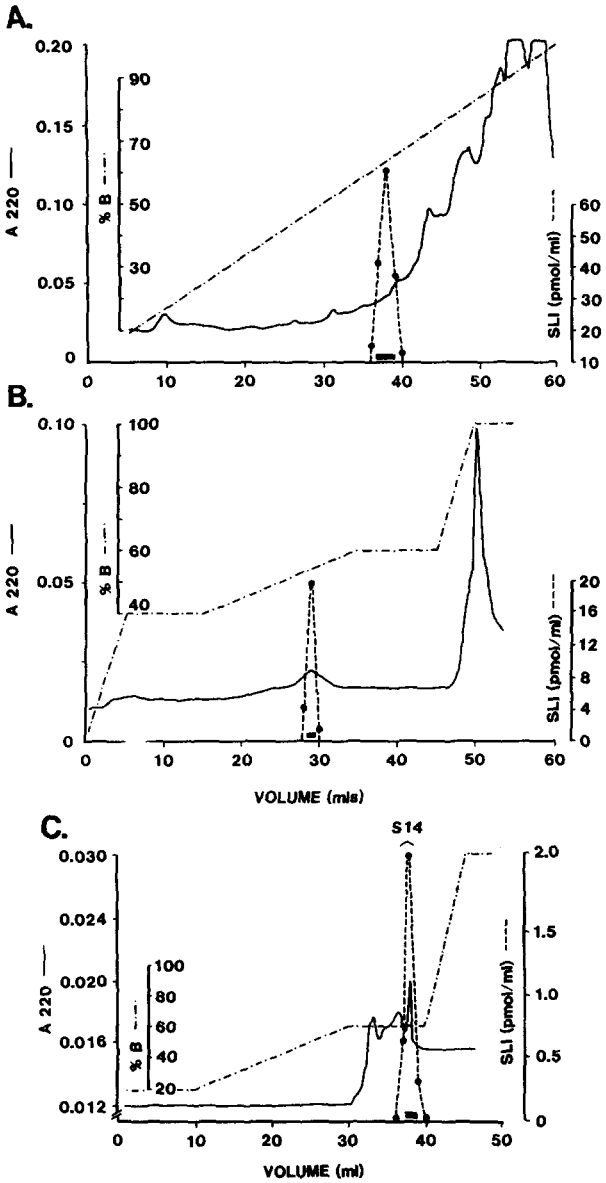

FIG. 23. Purification of frog retinal SLI by sequential HPLC on reverse phase C-18 Z-Module columns (A and B) and a C-18 Vydac column (C). The columns were equilibrated and calibrated as in Fig. 22. (From Takami *et al.*, 1985).

0.1% trifluoroacetic acid as buffer (Fig. 19). On the last phenyl HPLC column, a single sharp A220 peak was eluted and corresponded to the elution peak of SLI. This peak co-eluted with a synthetic S28 standard chromatographed on the same column. The final 1.7 nmol of purified SLI represented a cumulative recovery of 14.4% and a purification factor of 103,000-fold (Table 3). On automated Edman degradation amino acid sequencing of the purified retinal SLI (Fig. 20), the structure of the first 24 amino acids was determined to be identical to that of S28 (Table 4) purified from hog intestine (Pradayrol *et al.*, 1980) and from ovine (Esch *et al.*, 1980) and porcine hypothalamus (Schally *et al.*, 1980). The identity of the final 4 amino acids was confirmed by studies of antibody specificity and amino acid analysis (Table 5). A simultaneous partial purification of bovine brain SLI revealed HPLC peaks corresponding to both S28 and S14 (Fig. 21).

5.2. Frog Brain and Retina

The findings obtained with bovine retina conferred physiological relevance to functional studies in the mammalian retina employing S14 and S28, however, species differences in structure might limit interpretation of studies performed on retinas from submammalian species. The quantities of SLI extracted from submammalian retinas may be insufficient for any practical attempt at purification for the purpose of sequence analysis, however, our studies showing identical chromatographic properties on HPLC of purified SLI from retina and at least one molecular form of the peptide from brain indicated a possible solution to this problem. Detailed chemical characterization could be performed on minute quantities of purified retinal peptides and compared to their counterparts from brain which may be available in quantities sufficient for amino acid sequencing. With this logic in mind, we undertook the co-purification of frog brain and retinal SLI. We extracted the brains and retinas from 800 freshly killed frogs (*Rana pipiens*) in boiling 3% acetic acid and applied the extracts sequentially to affinity chromatography on Affi-Gel 10-antisomatostatin beads, multiple μ-Bondapak C-18 Z-module HPLC columns, and a final VYDAC C-18 HPLC column (Figs 22 and 23). Through these steps we were able to obtain 360 pmol of brain SLI purified 110,000-fold and 10 pmol of retinal SLI purified 93,000-fold (Table 6).

TABLE 6. *Recovery of Frog Brain and Retinal SLI at each Step of Purification*

Step	SLI (nmol)	Recovery (%) Step	Recovery (%) Cumulative	Purification (X)
Brain				
Extract	9.60	–	100	1
Affinity	6.60/3.30*	68.8	68.8	100
HPLC (Z-Module #1)	3.23	97.9	67.3	11,000
HPLC (Z-Module #2)	1.34	41.5	27.9	25,000
HPLC (Z-Module #3)	0.78	58.2	16.2	60,000
HPLC (Vydac)	0.36	46.2	7.5	110,000
Retina				
Extract	0.44	–	100	1
Affinity	0.10	22.7	22.7	200
HPLC (Z-Module #1)	0.06	60.0	13.6	9,000
HPLC (Z-Module #2)	0.02	33.3	4.5	66,000
HPLC (Vydac)	0.01	50.0	2.3	93,000

*Only 3.30 of the 6.60 nmol were further purified. From Takami *et al.*, 1985.

The finally purified SLI from brain and retina co-eluted in the same fraction which was also identical to the elution fraction of standard synthetic S14. Amino acid sequencing of frog brain SLI revealed it to be identical in structure to S14 (Table 7) but different from some other somatostatins isolated from submammalian species (Table 5). Because of the identical chromatographic characteristics of the co-purified retinal and brain SLI, we inferred that the structures were likely to be identical, hence functional studies performed with S14 on amphibian retina may be interpreted in a physiologically relevant light.

6. CONCLUSION

Somatostatin is but one example of the many polypeptides that have been proposed as neurotransmitters in the central and peripheral nervous systems. Our experiments to characterize the anatomy and biochemistry of somatostatin in the retina hopefully have provided the groundwork for future studies to determine the physiological function of retinal somatostatin. Such studies may help to elucidate the role of peptide neurotransmitters in normal and abnormal functions of the brain. Conversely, the brain and, more specifically, the retina has provided a convenient and useful model for examining the biochemistry and molecular biology of bioactive peptides such as somatostatin.

Acknowledgements — The work presented in this manuscript represents not only my own efforts but also those of David Marshak, Scott Basinger, and Mimi Takami. I am grateful for the secretarial assistance of Lori Ennis. Support for these studies was derived from National Institutes of Health grant R01 EY05205.

REFERENCES

AMES, A., III and NESBETT, F. B. (1981) *In vitro* retina as an experimental model of the central nervous system. *J. Neurochem.* **37**: 867–877.

ARIMURA, A., SATO, H., COY, D. H. and SCHALLY, A. V. (1975) Radioimmunoassay for GH-release inhibiting hormone. *Proc. Soc. exp. Biol. Med.* **148**: 784–789.

BAYLISS, W. M. and STARLING, E. H. (1902) Mechanism of pancreatic secretion. *J. Physiol. (Lond.)* **28**: 325–353.

BRAZEAU, P., VALE, W., BURGUS, R., LING, N., BUTCHER, M., RIVIER, J. and GUILLEMIN, R. (1973) Hypothalmic polypeptide that inhibits the secretion of immunoreactive pituitary growth hormone. *Science* **179**: 77–79.

BRECHA, N. (1983) Retinal neurotransmitters: histochemical and biochemical studies. In: *Chemical Neuroanatomy* (P. C. Emson, ed.) pp. 85–129. Raven Press, New York.

BUCKERFIELD, M., OLIVER, J., CHUBB, I. W. and MORGAN, I. G. (1981) Somatostatin-like immunoreactivity in amacrine cells of the chicken retina. *Neuroscience* **6**: 689–695.

CHIBA, T., PARK, J. and YAMADA, T. (1988) Biosynthesis of somatostatin in canine fundic D-cells. *J. Clin. Invest.* **81**: 282–287.

COSTA, M., PATEL, Y., FURNESS, J. B. and ARIMURA, A. (1977) Evidence that some intrinsic neurons of the

TABLE 7. *Amino Acid Sequences of S14 and Somatostatin of Lower Vertebrate Species*

Somatostatin	−8*	−7	−6	−5	−4	−3	−2	−1	1	2	3	4	5	6	7	8	9	10	11	12	13	14
S14									Ala	Gly	Cys	Lys	Asn	Phe	Phe	Trp	Lys	Thr	Phe	Thr	Ser	Cys
Frog brain									Ala	Gly	(Cys)	Lys	Asn	Phe	Phe	Trp	Lys	The	Phe	Thr	Ser	(Cys)
Anglerfish I									Ala	Gly	Cys	Lys	Asn	Phe	Phe	Trp	Lys	Thr	Phe	Thr	Ser	Cys
Anglerfish II									Ala	Gly	Cys	Lys	Asn	Phe	[Tyr]	Trp	Lys	[Gly]	Phe	Thr	Ser	Cys
Catfish pancreas	Asp	Asn	Thr	Val	Thr	Ser	Lys	Pro	[Leu]	[Asn]	Cys	[Met]	Asn	[Tyr]	Phe	Trp	Lys	[Ser]	[Arg]	Thr	[Ala]	Cys

*Amino acids are numbered from the amino terminus of S14. Parentheses denote that the cysteine residues in position 3 and 14 of frog brain somatostatin have yet to be confirmed. The amino acids that vary from those in the sequence of S14 are enclosed in square brackets. (From Takami *et al.*, 1986).

intestine contain somatostatin. *Neurosci. Lett.* **6**: 215 – 222.

DODD, J. and KELLY, J. S. (1978). Is somatostatin an excitory transmitter in the hippocampus? *Nature* **273:** 674 – 675.

EPELBAUM, J., BRAZEAU, P., TSANG, D., BRAWER, J. and MARTIN, J. B. (1977) Subcellular distribution of immunoassayable somatostatin in rat brain. *Nature* **273:** 161 – 163.

ESCH, F., BOHLEN, P., LING, N., BENOIT, R., BRAZEAU, P. and GUILLEMIN, R. (1980) Primary structure of ovine hypothalamic somatostatin-28 and somatostatin-25. *Proc. Natn. Acad. Sci. U.S.A.* **77:** 6827 – 6831.

ESKAY, R. L., LONG, R. T. and IUVONE, P. M. (1980) Evidence that TRH, somatostatin and substance P are present in neurosecretory elements of the vertebrate retina. *Brain. Res.* **196:** 554 – 559.

GUILLEMIN, R. (1976) Somatostatin inhibits the release of acetylcholine induced electrically in the myenteric plexus. *Endocrinology* **99:** 1653 – 1654.

HOKFELT, T., ELDE, R. P., JOHANNSON, O., LUFT, R. and ARIMURA, A. (1975a). Immunohistochemical evidence of the presence of somatostatin, a powerful inhibitory peptide, in some primary sensory neurons. *Neurosci. Lett.* **1:** 231 – 235.

HOKFELT, T., JOHANSSON, O., EFENDIC, S., LUFT, R. and ARIMURA, A. (1975b) Are there somatostatin nerves in the rat gut? Immunohistochemical evidence for a new type of peripheral nerve. *Experientia* **31:** 852 – 854.

HOKFELT, T., ELFVIN, L., ELDE, R., SCHULTZBERG, M., GOLDSTEIN, M. and LUFT, R. (1977). Occurrence of somatostatin immunoreactivity in some peripheral sympathetic nonadrenergic neurons. *Proc. Natn. Acad. Sci. U.S.A.* **74:** 3587 – 3591.

IOFFE, S., HAVLICEK, V., FRIESEN, H. and CHERNICK, V. (1978) Effect of somatostatin (SRIF) and L-glutamate on neurons of the sensori-motor cortex in awake habituated rabbits. *Brain Res.* **153:** 414 – 418.

IVERSON, L. L., IVERSON, S. D., BLOOM, F., DOUGLAS, C., BROWN, M. and VALE, W. (1978) Calcium dependent release of somatostatin and neurotensin from rat brains *in vitro*. *Nature* **273:** 161 – 163.

KANEKO, A. (1979). Physiology of the retina. *Annu. Rev. Neurosci.* **2:** 169 – 191.

KRISCH, B. (1978) Hypothalamic and extrahypothalamic distribution of somatostatin-immunoreactive elements in the rat brain. *Cell Tiss. Res.* **195:** 499 – 513.

KRULICH, L., DHARIVAL, A. P. S. and MCCANN, S. M. (1968) Stimulatory and inhibitory effects of purified hypothalamic extracts in growth hormone release from rat pituitary *in vitro*. *Endocrinology* **83:** 783 – 790.

LAKE, N. and PATEL, Y. C. (1980) Neurotoxic agents reduce retinal somatostatin. *Brain Res.* **181:** 234 – 236.

MARSHAK, D. W., REEVE, J. R., SHIVELY, J. E., HAWKE, D., TAKAMI, M. S. and YAMADA, T. (1983) Structure of somatostatin isolated from bovine retina. *J. Neurochem.* **41:** 601 – 606.

MARSHAK, D. and YAMADA, T. (1984) Characterization of somatostatin-like immunoreactivity in vertebrate retinas. *Invest. Ophthalmol. Vis. Sci.* **25:** 112 – 115.

MARSHAK, D., YAMADA, T. and STELL, W. K. (1984) Synaptic contacts of somatostatin-immunoreactive amacrine cells in goldfish retina. *J. comp. Neurol.* **225:** 44 – 52.

PARDRIDGE, W. M., EISENBERG, J. and YAMADA, T. (1985) Rapid sequestration and degradation of somatostatin analogues by isolated brain microvessels. *J. Neurochem.* **44:** 1178 – 1184.

PELLETIER, G., LABRIE, F., ARIMURA, A. and SCHALLY, A. V. (1974) Electron microscopic immunohistochemical localization of growth hormone-release inhibiting hormone (somatostatin) in the rat median eminence. *Am. J. Anat.* **140:** 445 – 450.

PRADAYROL, L., JORNVALL, J., MUTT, V. and RIBET, A. (1980) N-terminally extended somatostatin: the primary structure of somatostatin-28. *FEBS Letts.* **109:** 55 – 58.

RANDIC, M. and MILETIC, V. (1978) Depressant actions of methionine-enkephalin and somatostatin in cat dorsal root neurones activated by noxious stimuli. *Brain Res.* **152:** 196 – 202.

REICHLIN, S. (1983) Medical progress — Somatostatin. *New Engl. J. Med.* **309:** 1495 – 1501 (first part); 1556 – 1563 (second part).

RENAUD, L. P., MARTIN, J. B. and BRAZEAU, P. (1975) Depressant action of TRH, LH-RH, and somatostatin on activity of central neurones. *Nature* **255:** 233 – 235.

RORSTAD, O. P., BROWNSTEIN, J. J. and MARTIN, J. B. (1979) Immunoreactive and biologically active somatostatin-like material in rat retina. *Proc. Natn. Acad. Sci. U.S.A.* **76:** 3019 – 3023.

RORSTAD, O. and MARTIN, J. (1981) Neuropeptides in the visual system. In *Neuropeptides: Biochemical and Physiological Studies* (R. Miller, ed.), pp. 3 – 12. Churchill-Livingstone, New York.

SCHAEFFER, J. M., BROWNSTEIN, J. and AXELROD, J. (1977) Thyrotropin-releasing hormone-like material in the rat retina: changes due to environmental lighting. *Proc. Natn. Acad. Sci. U.S.A.* **74:** 3579 – 3581.

SCHALLY, A., HUANG, W. Y., CHANG, R., ARIMUA, A., REDDING, T., MILLAR, R., Hunkapiller, M. W. and HOOD, L. E. (1980) Isolation and structure of pro-somatostatin: a putative somatostatin precursor from pig hypothalamus. *Proc. Natn. Acad. Sci. U.S.A.* **77:** 4489 – 4493.

SHAPIRO, B., KRONHEIM, S. and PIMSTONE, B. (1979) The presence of immunoreactive somatostatin in rat retina. *Horm. Metab. Res.* **11:** 79 – 80.

STELL, W., MARSHAK, D., YAMADA, T., BRECHA, N. and KARTEN, H. (1980) Peptides are in the eye of the beholder. *Trends Neurosci.* **30:** 292 – 295.

STYNE, D. M., GOLDSMITH, P. C., BURSTEIN, S. R., KAPLAN, S. L. and BRUMBACH, M. M. (1977) Immunoreactive somatostatin and luteinizing hormone releasing hormone in median eminence synaptosomes of the rat: detection by immunohistochemistry and quantification by radioimmunoassay. *Endocrinology* **101:** 1099 – 1103.

TAKAMI, M., REEVE, J. R., JR, HAWKE, D., SHIVELY, J. E., BASINGER, S. and YAMADA, T. (1985) Purification of somatostatin from frog brain: Coisolation with retinal somatostatin-like immunoreactivity. *J. Neurochem.* **45:** 1869 – 1874.

YAMADA, T., MARSHAK, D., BASINGER, S., WALSH, J., MORLEY, J. and STELL, W. (1980) Somatostatin-like immunoreactivity in the retina. *Proc. Natn. Acad. Sci. U.S.A.* **77:** 1691 – 1695.

YAMADA, T. and BASINGER, S. (1981) Biosynthesis-like immunoreactivity by frog retinas *in vitro*. *J. Neurochem.* **39:** 1539 – 1546.